ECOHYDROLOGY
Ecohydrol. **5**, 297–305 (2012)
Published online 11 March 2011 in Wiley Online Library
(wileyonlinelibrary.com) DOI: 10.1002/eco.214

Soil moisture and ecosystem function responses of desert grassland varying in vegetative cover to a saturating precipitation pulse

Erik P. Hamerlynck,* Russell L. Scott and Jeffry J. Stone
USDA-ARS Southwest Watershed Research Center, 2000 E. Allen Road, Tucson, AZ 85719, USA

ABSTRACT

A critical linkage between hydrological and ecological processes is plant cover, yet the ecosystem-level responses of aridland systems of varying plant cover to extreme precipitation events, predicted to increase in the future, have not been well studied. We tracked volumetric soil water ($\theta_{15\ cm}$) across the entire summer monsoon season, and ecosystem evapotranspiration (ET), net ecosystem carbon dioxide exchange (NEE), ecosystem respiration (R_{eco}), gross ecosystem photosynthesis (GEP), and leaf-level net carbon assimilation (A_{net}) and stomatal conductance to water vapour (g_s) for 30 days in high-cover (*ca.* 50%) and low-cover (*ca.* 23%) plots in response to a runoff generating experimental rainfall. For 35 days following the pulse, $\theta_{15\ cm}$ was 2·5% higher in high-cover plots compared to low-cover values, with identical soil drying rates between cover conditions. After $\theta_{15\ cm}$ converged to similar values between cover conditions, dry-down rates were longer in low-cover plots. ET and g_s did not differ between plots. For 7 days after the pulse, slower A_{net} development in some grass species compared to rapid development by the canopy dominant, Lehmann's lovegrass, may have resulted in similar GEP between low- and high-cover plots. After this, GEP and R_{eco} were higher and increased in parallel in high-cover plots. In low-cover plots, R_{eco} levelled at +21 days, resulting in similar NEE to high-cover plots, even though GEP was lower. These findings suggest that low biomass in low-cover areas may constrain R_{eco} and lead to more evenly distributed productivity across semiarid grasslands following large, infrequent precipitation events. Published in 2011. This article is a US Government work and is in the public domain in the USA.

KEY WORDS leaf area index; net ecosystem carbon exchange; photosynthesis; respiration; runoff

Received 12 February 2010; Accepted 15 February 2011

INTRODUCTION

Some climate change predictions for western North America predict an overall decrease in annual precipitation due to an increase in more widely spaced, larger high intensity events (Easterling *et al*., 2000a,b; Christensen and Hewitson, 2007; Seager *et al*., 2007). Such altered rainfall regimes are expected to have widespread impacts on ecosystem processes and services (Gerten *et al*., 2008; Knapp *et al*., 2008). If larger and less frequent storms become more common, 'super-saturating' events may also increase in frequency, a phenomenon that would be of particular importance in arid systems where there is the probability that much of the annual rainfall can occur in any single rainfall event (Noy-Meir, 1973; Comrie and Broyles, 2002; Sheppard *et al*., 2002). Large, infrequent precipitation events are highly important, in that they trigger large runoff events, promote rapid and extensive hillslope erosion, facilitate deep soil and ground water recharge, and can reorganize landscape soil and hydrological features (Seyfried *et al*., 2005; Goodrich *et al*., 2008; Nimmo *et al*., 2009), often with long-lasting consequences to aridland plant community structure and function (Wondzell *et al*., 1996; Ogle and Reynolds, 2004; Knapp *et al*., 2008; Robertson *et al*., 2010).

A fundamental linkage between rangeland hydrological and ecosystem processes is the degree of vegetative cover. The degree and spatial distribution of vegetation cover strongly mediates interception, infiltration, runoff, and patterns of sediment transport in aridland watersheds (Sanchez and Puigdefabregas, 1994; Domingo *et al*., 1998; Gómez-Plaza *et al*., 2001; Ludwig *et al*., 2005; Nearing *et al*., 2005; Puigdefabregas, 2005; Scanlon *et al*., 2005). In grasslands, greater cover is usually associated with higher seasonal net productivity and enhanced soil moisture, but may also induce light limitations due to self-shading and feedbacks on nutrient cycling (Knapp and Seastedt, 1986; Knapp *et al*., 1993; Ryel *et al*., 1993; Fay *et al*., 2003; English *et al*., 2005). In more water-limited grasslands, widely spaced large precipitation events have been found to enhance productivity to a greater extent than in more mesic grasslands, in part by alleviating water stress over longer post-storm time periods (Fay *et al*., 2003, 2008; Heisler-White *et al*., 2008, 2009), and could thus be expected to enhance feedbacks associated with greater cover on ecosystem carbon balance. A critical need, therefore, is to directly partition grassland net ecosystem carbon exchange into its constituent fluxes in grassland plots varying in degree of cover in response to an extreme rainfall event.

* Correspondence to: Erik P. Hamerlynck, USDA-ARS Southwest Watershed Research Center, 2000 E. Allen Road, Tucson, AZ 85719, USA.
E-mail: erik.hamerlynck@ars.usda.gov

Here, we present the results of a study assessing the ecosystem and leaf-level gas exchange and volumetric soil moisture responses of a desert grassland varying in vegetative cover to an experimental saturating event. Previous pulse experiments in rain-out shelters have shown that the greatest response to precipitation in desert grassland follows release from pre-summer monsoon drought stress, when the grassland undergoes a rapid reorganization from a modest carbon source to a strong carbon sink in the first week following rainfall (Huxman *et al*., 2004; Potts *et al*., 2006). Net ecosystem carbon dioxide exchange (NEE) reflects the balance between ecosystem respiration (R_{eco}) and gross ecosystem photosynthesis (GEP), both of which show distinct responses to variation in soil moisture and temperature (Flanagan and Johnson, 2005; Potts *et al*., 2006; Patrick *et al*., 2007; Jenerette *et al*., 2008). R_{eco} in many grasslands is generally dominated by belowground root respiration (Knapp *et al*., 1998; Flanagan *et al*., 2002), though in arid systems, large and rapid transient increases in R_{eco} in response to rainfall following prolonged dry periods are attributed to microbial activity (Huxman *et al*., 2004; Jarvis *et al*., 2007). GEP is a function of both the development of leaf-level photosynthetic capacity and canopy development (Ryel *et al*., 1993; Potts *et al*., 2006). We specifically expected:

1. Volumetric soil moisture (θ) levels and dynamics would be similar between high- and low-cover plots, as runoff generating rainfall should be sufficient to overcome any differences in canopy interception (Rodriguez-Iturbe *et al*., 1999).
2. Development of leaf-level photosynthesis (A_{net}) and stomatal conductance to water vapour (g_s) to be similar between high- and low-cover plots because of high, similar water availability (Ignace *et al*., 2007). As a result, we expected that canopy-level photosynthesis, i.e. GEP scaled to leaf level using leaf area index (GEP_{lai} = GEP/LAI) to be identical between high- and low-cover conditions.
3. High-cover plots to have higher evapotranspiration (ET) and more negative NEE, the latter reflecting higher GEP per unit R_{eco}. Soil respiration in semiarid grasslands is suppressed in widely spaced large rainfall treatments, whereas leaf-level photosynthesis is not (Fay *et al*., 2008). With more extensive leaf coverage, GEP could therefore be expected to be greater in high-cover plots, resulting in more negative NEE.

MATERIALS AND METHODS

Field work took place from 21 June to 24 July 2008 at the Kendall Grassland site (109°56′28″W, 31°44′10″N, 1526 m asl), located in the Walnut Gulch Experimental Watershed (WGEW), *ca*. 11 km east of Tombstone, AZ. Kendall Grassland is a desert grassland, historically dominated by black grama (*Bouteloua eripoda*), side-oats grama (*B. curtipendula*), hairy grama (*B. hirsuta*), tanglehead (*Heteropogon contortus*), curly mesquite (*Hilaria berlangeri*), and the exotic South African bunchgrass, Lehmann lovegrass (*Eragrostis lehmanniana*). Soils at the Kendall rainfall simulation site are in the Elgin–Stronghold complex and are dominated by Stronghold series soils, which are gravelly fine sandy loams, classified as coarse-loamy, mixed, superactive thermic Ustic Haplocalcids (Rhoton *et al*., 2007; Emmerich and Verdugo, 2008). Typical precipitation thresholds for sustained ecosystem carbon uptake were 23 mm (Emmerich and Verdugo, 2008), with typical growing season (July to September) accumulations of 200–220 mm (Scott *et al*., 2000). Following protracted drought from 2002 to 2006, there was a marked increase in the abundance of the invasive Lehmann lovegrass across the rainfall simulation plots and the Kendall grassland watershed (Stone, unpublished data; Moran *et al*., 2009).

The Walnut Gulch Rainfall Simulator (WGRS; Paige *et al*., 2003) was used to apply water on four 2 × 6 m plots. The WGRS is an oscillating boom simulator that uses four VeeJet 80100 nozzles evenly spaced on the boom to apply water at variable intensities ranging from 25 to 180 mm h^{-1}. The simulation run sequences were as follows; all plots had a dry run consisting of 45-min application at 65 mm h^{-1} to initial soil moisture conditions. A wet run was initiated 45 min after the cessation of runoff from the dry run and consisted of a sequence of application rates from 65 to 180 mm h^{-1} in increasing increments of intensity. For the wet run, the application rates were changed after runoff had reached steady state for at least 5 min at a given rainfall intensity, leading to different total rainfall application totals (Table I). Runoff depth at the down-slope outlet of a plot was measured using an electronic staff gauge and a pre-calibrated flume and was converted to a discharge using the flume's stage–discharge relationship. Runoff depth measurements were taken at 1-min intervals during the rise of the hydrograph and at 2- to 3-min intervals during steady state runoff. Rainfall intensities were based on a yearly calibration of the simulator.

Before the dry run, canopy and ground cover were measured using a point frame on a 15 × 20-cm grid for a total of 400 points. Canopy cover was recorded to species if possible, or else classified as grass, shrub, or forb. Relative dominance (% of plant canopy) of the invasive South African bunchgrass, all native bunch grasses, and broad-leaved forbs was estimated by dividing the sum of hits for each plant by the total number of plant hits for each plot. Ground cover was recorded as rock + gravel (>2 mm), litter, vegetative base, and bare soil and was measured both under and between canopy cover. Litter was defined as dead plant material in contact with the soil surface. Total vegetative canopy cover was 20–26% in low-cover plots and 43–56% in high-cover plots, however, with the former dominated by the invasive South African bunchgrass, Lehmann's lovegrass (Table I). Ground cover was similar in terms of litter and plant basal area, while low-cover plots had substantially more rock cover in the high-cover runoff plots. Total rainfall applied to the four runoff plots was *ca*. 75–93%

of long-term summer growing season averages (Scott *et al*., 2000; Emmerich and Verdugo, 2008).

ECH_2O-10 (Decagon Devices, Pullman, WA, USA) probes were used to measure volumetric soil moisture at 15 cm below the soil surface ($\theta_{15\ cm}$), the depth to which our grasses root *ca.* 85% of their root biomass (Gibbens and Lenz, 2001). Probes were installed horizontally in the faces of small slit-trenches at least 1 week prior to the rainfall simulation. $\theta_{15\ cm}$ data were recorded every 30 min, until the day of rainfall simulation, when sampling frequency was increased to 5 min for 48 h to capture wetting front infiltration rates to 15 cm (mm min^{-1}; estimated by noting the difference in time following start of rainfall for the dry run to first significant departure from initial $\theta_{15\ cm}$), maximum wet-up rate ($\theta_{15\ cm}$ min^{-1}) during the dry run, and the 24-h drying decay rate following cessation of rainfall simulation for the wet run. Maximum wet-up rates were determined from the slopes of linear regressions to the best fit portion of the initial 45-min wet-up, and 24-h drying decay rates were estimated using nonlinear regressions of exponential decay ($y = y_0 + a \times e^{-bx}$, with decay rates estimated as $1/b$; SigmaPlot v10.0, SPSS, Chicago, IL, USA). After this, 30-min data recording intervals were re-established to track $\theta_{15\ cm}$ for the ecosystem and leaf-level gas-exchange sampling and rest of the growing season. To determine whether soil drying rates were different between low- and high-cover plots, e-folding times (in days) were estimated for $\theta_{15\ cm}$ following five storm events followed by interstorm periods of at least 5 days. To do this, daily average values of $\theta_{15\ cm}$ for each interstorm period were estimated and then normalized by dividing the maximum daily average value occurring on the first day following the storm. Nonlinear regressions of exponential decay ($y = a \times e^{-bx}$; SigmaPlot v10.0) were generated for $\theta_{15\ cm}$ pooled for three θ probes in each plot for each storm. The e-folding times were calculated as $1/b$, and indicate how long it takes $\theta_{15\ cm}$ to reduce to 33% of the maximum starting values.

The WGEW rainfall simulator was designed for highly precise measurements of rainfall intensity, infiltration, runoff, and sediment discharge rates for large, hillslope-scale representative plots (Paige *et al*., 2003) and was not designed for large numbers of replicated plots. Therefore, we have used the large 12-m^2 experimental runoff plots as the landscape context in which we compared mid-morning (9 : 00 to 11 : 00 MST) ecosystem CO_2 and water vapour fluxes of high- and low-cover 0·75 × 0·75-m gas-exchange plots located within each runoff plot. CO_2 and H_2O fluxes were estimated by measuring changes in CO_2 and H_2O concentrations with an open-path infrared gas analyzer (IRGA; LI-7500, LiCOR Instruments, Lincoln, NE, USA) following enclosure with a 0·75 × 0·75 × 0·75-m (0·422 m^3) chamber of tightly sewn polyethylene (Shelter Systems, Aptos, CA, USA) held taut within a tent frame of polyvinyl chloride (PVC) pipe. Chamber material allowed 92% of photosynthetically active radiation to pass into the plots, while allowing infrared radiation to escape (Potts *et al*., 2006). Eight gas-exchange plots were established, two in each large runoff plot, each centred over a $\theta_{15\ cm}$ probe, and encompassing vegetative cover typical of the large runoff plot they were located in. A fan attached to the tripod holding the IRGA ensured atmospheric mixing after enclosure and sealing the chamber base with a chain. Chamber air was mixed for at least 30 s prior to flux measurements, which lasted *ca*. 90 s, with the chamber on the plot for 2–3 min. The chamber was removed, aerated for 0·5–1 min, then replaced over the plot, sealed, and shaded with a blanket for 2 min prior to repeating measurements in the dark. Photosynthetic photon flux density (PPFD) in the shaded chamber was under 5 μmol m^{-2} s^{-1}. Tags driven into the soil at each corner of the chamber frame ensured exact repositioning. Ambient light fluxes allowed estimation of NEE and ET; dark measurements gave R_{eco} and, by calculation, GEP [$GEP = -1 \times (NEE - R_{eco})$]. LAI for each gas-exchange plot measured using a LiCOR 2000 canopy analyzer (LiCOR Instruments) was used to scale GEP to leaf-level estimate canopy-level photosynthesis (GEP_{lai} = GEP/LAI). LAI was estimated under constant overcast conditions for each gas-exchange plot and averaged across five below-canopy samples for each plot. LAI was measured 1 day prior to and 15 days after water application and did not differ substantially between these two periods, so all observations were pooled to give a representative LAI value for each gas-exchange plot.

Concurrent with ecosystem measurements, leaf-level photosynthetic gas exchange of net photosynthetic carbon assimilation (A_{net}) and g_s were measured using a portable photosynthesis system (Li-6400, LiCOR Instruments). Measurements were made on individual leaf blades of two Lehmann's lovegrass plants and any co-occurring native bunch grass, usually low woolly grass (*Dasyochloa pulchella*) or black grama (*Bouteloua eriopoda*), and each was averaged per gas-exchange plot. Cuvette CO_2 was held at 380 ppm, with a PPFD of 1500 μmol m^{-2} s^{-1} provided by a red–blue high intensity light source attached to the cuvette and measured with an internal gallium arsenide PPFD sensor. In all cases, external PPFD was near, or exceeded, internal cuvette PPFD. Cuvette temperature was held from 30 to 34 °C by setting block temperature of an attached Peltier-cooling block to 30 °C. After leaves equilibrated for *ca*. 2 min, five consecutive measures were recorded and averaged. Leaf-level and ecosystem exchange measurements were made during the peak period for diurnal physiological activity throughout the summer growing season (Ignace *et al*., 2007), and ecosystem-level fluxes at this time are highly correlated with diurnally integrated measures (Hamerlynck *et al*., 2010).

Ecosystem and leaf-level measurements were made 24 h prior to pulse application (−1 day), then repeated 1, 2, 3, 4, 7, 15, 21, and 30 days after rainfall application. A split-plot repeated-measures analysis of variance (RM-ANOVA, Statistix v8.0, Analytical Software, Tallahassee, FL, USA) tested for differences in NEE, R_{eco}, GEP, and GEP_{lai} with a whole-plot (between treatment) effect of cover type (high-cover vs low-cover), using

Table I. Vegetative cover, simulated rainfall amounts, and associated surface hydrological responses of the individual low- and high-cover desert grassland experimental runoff plots.

	Low 1	Low 2	High 1	High 2
Slope (%)	11.8	11.2	9.6	10.7
Aspect (°N)	311	311	305	296
Canopy cover (%)	26	20	56	43
% Lehmann's lovegrass	62.1	64.2	94.7	95.5
% Native grasses	23.0	26.9	1.0	2.5
% Forbs	14.9	9.0	4.3	2.0
Litter cover (%)	43	35	47	41
Rock cover (%)	24	31	16	18
Basal cover (%)	3	4	6	4
LAI (m^2 m^{-2})	0.29 (0.069)	0.25 (0.044)	0.52 (0.051)	0.42 (0.099)
Rain (mm)	188	204	189	166
Runoff (mm)	118	129	108	130
Infiltration (mm)	69	76	81	35
Wetting front rate (mm min^{-1})	11.0	19.0	14.0	9.0
Maximum wet-up rate (θ min^{-1})	1.03	1.00	0.79	0.84
24-h drying decay rate (h)	5.09	4.36	7.59	5.44

LAI values are the mean and standard errors of four measurements in two gas-exchange plots within each runoff plot.

the type-by-replicate interaction as the F-test error term ($n = 4$ for each cover type). Day of sampling (−1, 1, 2, 3, 4, 7, 21, and 30 days) and time-by-cover type interaction were the sub-plot, within-treatment effects, using the type-time-replicate as F-test error term. For leaf-level analyses, native bunchgrasses did not occur in the high-cover gas-exchange plots in sufficient numbers to allow a full factorial ANOVA design for comparing photosynthetic responses of native grasses and the invasive Lehmann's lovegrass in high- and low-cover conditions. Thus, we used a split-plot RM-ANOVA to compare A_{net} and g_s of high-cover lovegrass, low-cover lovegrass, and low-cover native bunchgrasses, using these cover−species combinations as the whole-plot factor, with the combination-by-replicate interaction as the F-test error term. Sampling date and time-by-combination interactions were the within-treatment effects, using the combination-by-time-by-replicate interaction as the F-test error term. For both ecosystem and leaf-level RM-ANOVA, the two-way interactions were of specific interest, as these indicate treatment-specific responses over time. α-adjusted general linear contrasts (t-test) compared specific contrasts that may underlie any significant two-way interaction effects.

Carbon-gain/cost relationships established by regressing +4 to +30 days GEP against R_{eco} by comparing slopes and elevations of low- and high-cover plots (Linear regression, Statistix 8·0), with the intercept forced through the origin, as GEP cannot be negative.

RESULTS

Both low-cover runoff plots showed very similar partition of rainfall, averaging 63% precipitation lost to runoff and 34% to soil infiltration, whereas high-cover runoff plots had similar wetting front infiltration rates, but low-cover plots showed greater changes in $\theta_{15\ cm}$ during the dry run rainfall application, as well as more rapid 24-h drying rates (Table I).

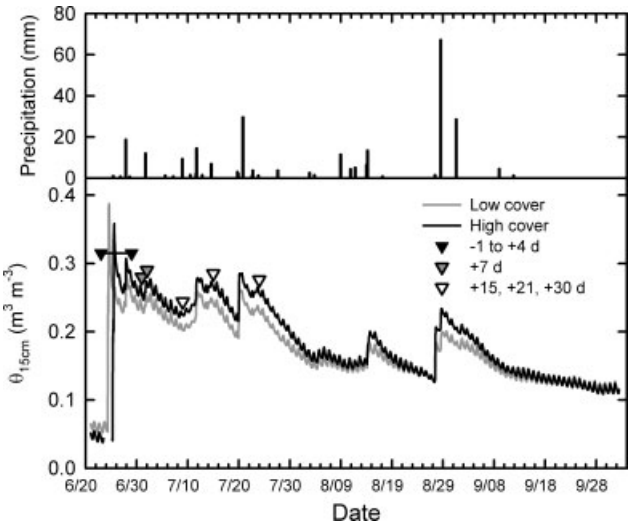

Figure 1. Monsoon season precipitation and volumetric soil water content at mean rooting depth ($\theta_{15\ cm}$) of high- and low-cover desert grassland hillslope plots following an experimental runoff generating precipitation pulse. Inverted triangles show ecosystem and leaf-level gas-exchange sampling dates.

Immediately following rain application, $\theta_{15\ cm}$ was higher in low-cover plots (*ca.* 38%) compared to high-cover plots (34%), but rapidly fell to levels 2–2·5% below high-cover plots 24-h following the rainfall application, a difference that was maintained from 26 June to 3 August (Figure 1). Following the first two large natural rainfall in this period, $\theta_{15\ cm}$ e-folding times of high- and low-cover plots were similar (2–8 July and 15–19 July; Figure 2), but began to diverge following 21 July, with lower e-folding times in high-cover plots (Figure 2). Low-cover plot $\theta_{15\ cm}$ e-folding times rose over the last three soil drying periods, whereas high-cover e-folding

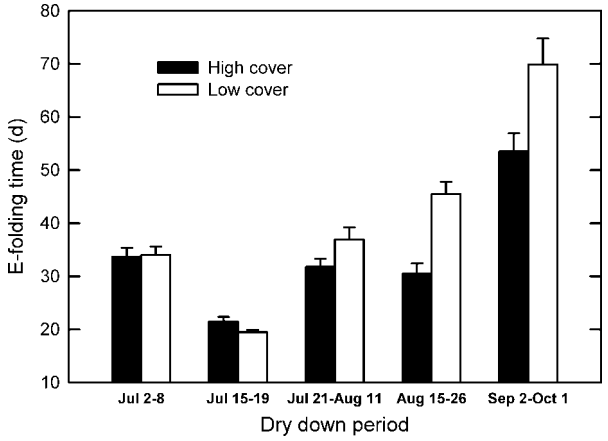

Figure 2. E-folding times of high- and low-cover plot $\theta_{15\ cm}$ for five soil drying periods following an experimental saturating precipitation pulse; note that the last three dry downs occurred after convergence in $\theta_{15\ cm}$ in high- and low-cover plots (Figure 1).

times only increased over the protracted drying period following the last monsoon season rainfall (2 September to 1 October; Figure 2).

Differences in leaf-level photosynthesis (A_{net}) and stomatal conductance (g_s) between low-cover Lehmann's lovegrass, low-cover native grasses, and high-cover lovegrass varied significantly through time after pulse application ($F_{16,66} = 3{\cdot}58$ and $3{\cdot}19$ for A_{net} and g_s, respectively, $p < 0{\cdot}001$). These significant two-way interactions resulted due to several reasons. First, in the period immediately following the pulse (+1 to +4; Figure 3), A_{net} in low-cover lovegrass plants was significantly higher than in lovegrass in high-cover gas-exchange plots (general linear contrast $t = -2{\cdot}34$; $p = 0{\cdot}0218$), whereas g_s between these did not differ ($t = -1{\cdot}14$; $p = 0{\cdot}154$; Figure 3). Also at this time, lovegrass A_{net} and g_s were significantly higher than in native grasses growing in low-cover gas-exchange plots ($t = 3{\cdot}12$ and $5{\cdot}38$ for A_{net} and g_s, respectively; $p < 0{\cdot}001$; Figure 3). From +7 to +30 days after the pulse, A_{net} was similar between all species–cover combinations ($t = 1{\cdot}90$; $p = 0{\cdot}061$), but g_s in native grasses in low-cover gas-exchange plots was significantly higher than in low- and high-cover lovegrass ($t = -2{\cdot}92$; $p = 0{\cdot}005$; Figure 3). LAI-adjusted GEP (GEP_{lai}) did not differ between gas-exchange plots ($F_{1,6} = 3{\cdot}42$; $p = 0{\cdot}114$) with no significant cover-by-time interaction ($F_{8,47} = 0{\cdot}67$; $p = 0{\cdot}718$). GEP_{lai} was very low and identical between high- and low-cover plots prior to and up to +15 days following the pulse, then rose steadily and converged with leaf-level A_{net} on +30 days (Figure 3).

NEE did not differ between high- and low-cover gas-exchange plots pooled across the pulse experiment ($F_{1,6} = 0{\cdot}156$; $p = 0{\cdot}258$) with no cover-by-time interaction ($F_{8,48} = 0{\cdot}179$; $p = 0{\cdot}102$; Figure 4). NEE varied significantly throughout the study period ($F_{8,48} = 82{\cdot}9$; $p < 0{\cdot}0001$) due to sharp increases in NEE immediately following the pulse, concurrent with a twofold increase in R_{eco} (Figure 4). NEE declined to compensation by +4 days and remained below compensation

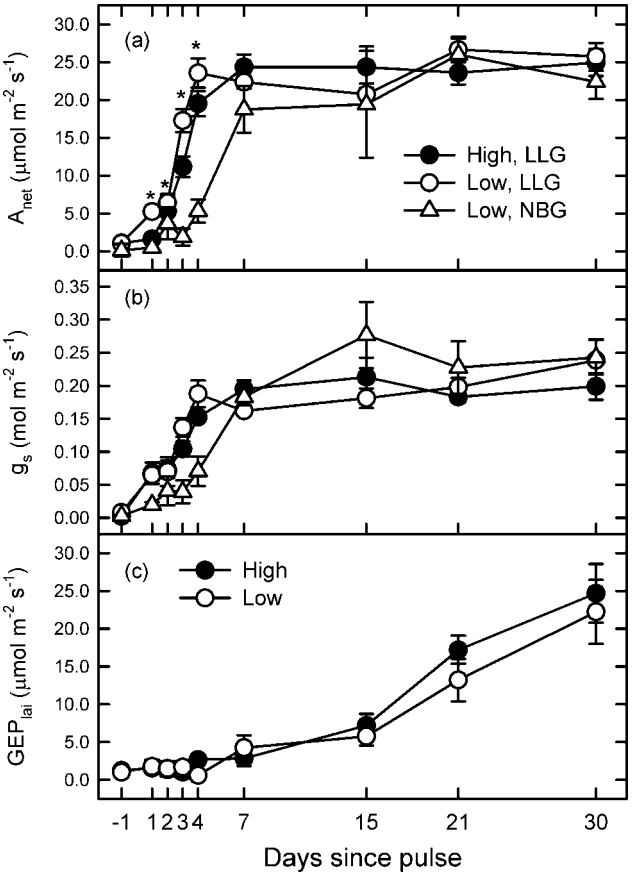

Figure 3. Pre- and post-pulse leaf-level (a) net photosynthesis and (b) stomatal conductance of water vapour of Lehmann's lovegrass (LLG) and native bunch grasses (NBG), and (c) canopy-level photosynthesis (GEP_{lai}) in desert grassland plots varying in vegetative cover. Each symbol is the mean of four independent measurements, error bars indicate ±1 SE, and asterisks indicate significant differences between lovegrass in high- and low-cover gas-exchange plots (General linear contrast *t*-test).

from +7 to +30 days (Figure 4). R_{eco} and GEP did not differ between high- and low-cover gas-exchange plots pooled across the study ($F_{1,6} = 5{\cdot}06$; $p = 0{\cdot}066$ and $F_{1,6} = 3{\cdot}42$; $p = 0{\cdot}114$, respectively) but did have significant cover-by-time interaction effects ($F_{8,47} = 3{\cdot}31$; $p = 0{\cdot}004$ for R_{eco} and $F_{8,47} = 3{\cdot}19$; $p = 0{\cdot}006$ for GEP, respectively). For R_{eco}, this was due to R_{eco} in high-cover plots peaking at +1 day following rainfall application, when R_{eco} in high-cover plots had increased over twofold from pre-pulse levels, followed by steady declines from +3 to +7 days (Figure 4). In low-cover plots, R_{eco} peaked at +3 days, then declined to levels below high-cover plots to +4 days, then converged with high-plot levels on +7 days (Figure 4). As a result, R_{eco} pooled across +1 to +4 days did not differ significantly between gas-exchange plots ($t = 0{\cdot}83$; $p = 0{\cdot}408$). From +15 to +30 days, R_{eco} in both rose, but to markedly higher levels in high-cover gas-exchange plots, which continually increased to +30 days, whereas R_{eco} in low-cover plots stabilized by +21 days (Figure 5). As a result, R_{eco} in high-cover plots was higher than low-cover R_{eco} across this period ($t = 4{\cdot}53$; $p < 0{\cdot}001$; Figure 4). The two-way interaction in GEP was due to divergence from similar GEP between cover types up to

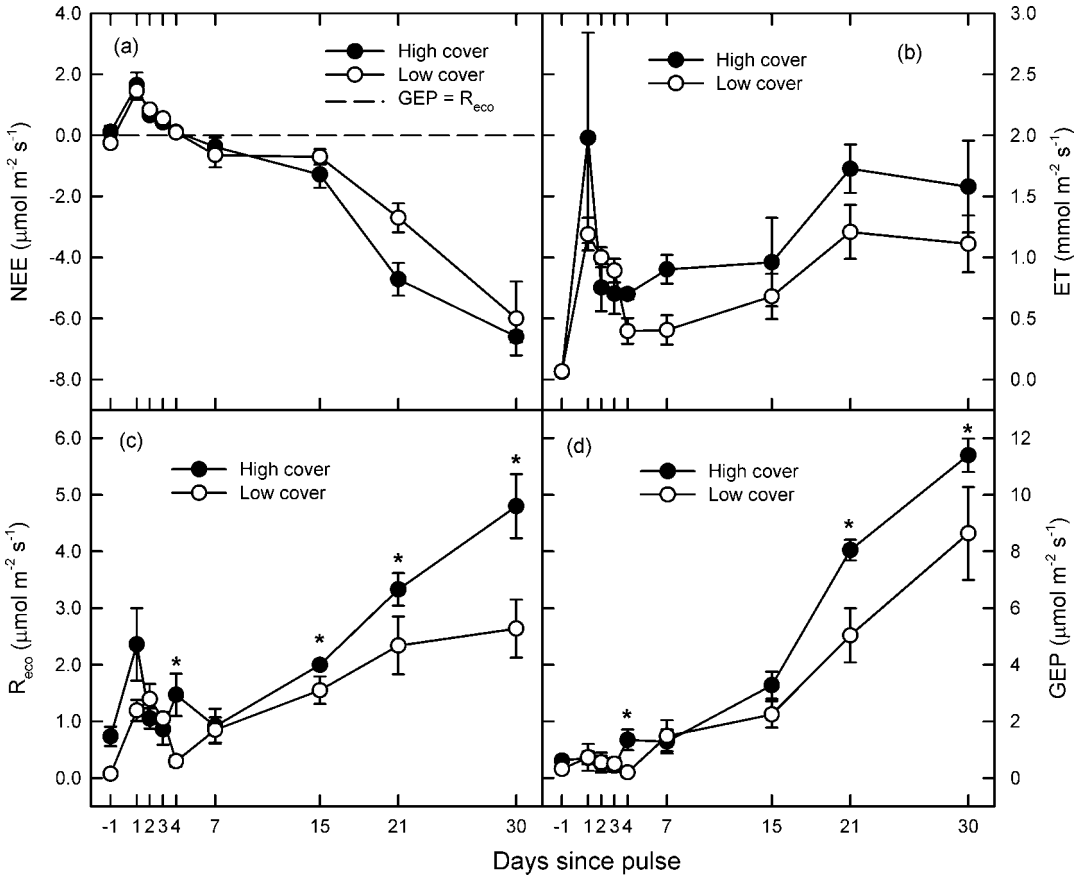

Figure 4. Pre- and post-pulse (a) net ecosystem CO_2 exchange, (b) plot-level evapotranspiration, (c) ecosystem respiration, and (d) gross ecosystem photosynthesis of 0·75 × 0·75 m gas-exchange plots varying in vegetative cover. Each symbol is the mean of four independent measurements, error bars indicate ±1 SE, and asterisks indicate date-specific high- and low-cover differences (General linear contrast *t*-test).

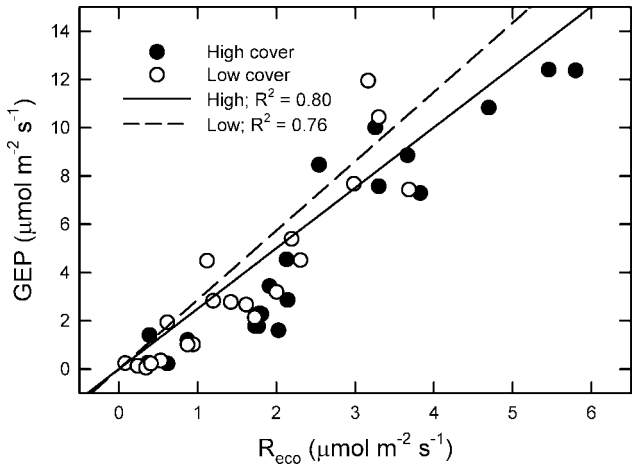

Figure 5. Relationship of gross ecosystem photosynthesis and ecosystem respiration of high- and low-cover desert grassland plots from +4 to +30 days following an experimental saturating precipitation pulse.

+7 days, after which high-cover gas-exchange plots had higher GEP compared to low-cover plots ($t = 4{\cdot}10$; $p < 0{\cdot}001$; Figure 4). Whole-plot ET varied across the study period ($F_{8,47} = 6{\cdot}57$; $p < 0{\cdot}0001$), with ET peaking at +1 day, then declining, but with ET still greater than pre-pulse levels, by +2 days (high-cover) or +4 days (low-cover; Figure 4). ET pooled across the study was greater in high-cover plots (1·07 mmol m^{-2} s^{-1} + 0·143 SE), but these did not significantly differ from low-cover ET (0·77 mmol m^{-2} s^{-1} + 0·08 SE; $F_{1,6} = 4{\cdot}22$; $p = 0{\cdot}086$), with interaction effect ($F_{8,47} = 0{\cdot}82$; $p = 0{\cdot}589$).

GEP and R_{eco} were positively correlated when pooled across high- and low-cover gas-exchange plots (GEP = 2·251 × R_{eco}; $R^2 = 0{\cdot}92$; $F_{1,39} = 491{\cdot}36$; $p < 0{\cdot}0001$) and within each cover type (Figure 5). High- and low-cover gas-exchange plots had similar GEP/R_{eco} slopes (2·5 for high-cover and 2·87 for low-cover; $F_{1,36} = 0{\cdot}94$; $p = 0{\cdot}34$), but low-cover plots had significantly higher GEP per unit R_{eco} across the study, as indicated by a significant difference in slope elevations ($F_{1,37} = 7{\cdot}38$; $p = 0{\cdot}010$; Figure 5).

DISCUSSION

The volumetric soil moisture data showed that the artificial saturating pulse had an extensive residence time, as seen when soil moisture of low- and high-cover plots responded to wetting and drying in a similar manner (Figures 1 and 2), suggesting the experimental pulse supplemented ambient precipitation for about 35 days. The consistently higher θ in high-cover plots after wetting and initial gravity drainage may be due to reduction in soil evaporative losses (English *et al.*, 2005) or higher field capacity. In addition to drying down at similar rates (Figure 2), high-cover and low-cover runoff plots

responded similarly to rewetting (Figure 1). These high antecedent moisture conditions likely resulted in minimal responses in leaf-level photosynthesis and in NEE (and its constituent fluxes) following any natural rainfall (Potts *et al*., 2006; Ignace *et al*., 2007). After $\theta_{15\ cm}$ converged between high- and low-cover runoff plots (Figure 1), soils in these plots behaved differently in drying (Figure 2) and in response to rewetting (Figure 1). These may reflect imposition of a hysteresis effect following more severe drying that had been minimized previously by the saturating pulse (Hogarth *et al*., 1989). In addition, the more rapid drying times in high-cover plots later in the season may reflect plant water utilization following precipitation events sufficient for prolonged plant activity (Emmerich and Verdugo, 2008).

It was surprising that ET averaged across the study period did not significantly differ between high- and low-cover gas-exchange plots (Figure 4), given that bare-soil evaporation contributions to ET decay rapidly and are minimal after only a few days following rainfall events in semiarid rangelands (Huxman *et al*., 2004; Scott *et al*., 2006; Moran *et al*., 2009). However, the large nature of the pulse may have swamped any differences in soil and canopy evaporation during the first 4 days, when $\theta_{15\ cm}$ was high (Figure 1) and ET was similar between high- and low-cover conditions (Figure 4). Analyzing only the +4 to +30 days period, when leaves of the canopy dominant, Lehmann's lovegrass, had steady state g_s (Figure 3), ET was significantly higher in high-cover plots compared to low-cover gas-exchange plots ($F_{1,6} = 10{\cdot}30$; $p = 0{\cdot}018$; Figure 4). This suggests that transpiration (T) contributions to ET in high-cover plots came from more extensive leaf area (Table I) and not higher stomatal conductance. If this is the case, the faster dry-down times apparent in high-cover runoff plots over the last three drying periods (Figure 2) may reflect greater plant water use; indeed, our final ET sampling was made on the third day of this period and ET was markedly higher in high-cover gas-exchange plots (Figure 3), but concurrent leaf-level or whole-plot data are lacking to confirm if this was the case across the final two drying periods of the season.

During the 30 days post-pulse period when NEE was measured, water was essentially non-limiting (Figure 1); there were no differences in the NEE between high- and low-cover gas-exchange plots (Figure 4). Even analyzing +4 to +30 days, as done above for ET, low- and high-cover NEE plots did not differ ($F_{1,6} = 0{\cdot}02$; $p = 0{\cdot}88$), with no cover-by-time interaction ($F_{2,24} = 0{\cdot}48$; $p = 0{\cdot}75$). Once NEE reached compensation by +4 days, R_{eco} in high-cover gas-exchange plots rose continually from +7 to +30 days, whereas rates in low-cover plots levelled off at +21 days and were about half of R_{eco} rates in high-cover plots (Figure 4). Concurrently, lower GEP in low-cover plots paralleled increases in high-cover plot GEP, resulting in similar NEE (Figure 4). As in Huxman *et al*. (2004) and Potts *et al*. (2006), A_{net} achieved peak levels well before NEE or GEP (Figures 3 and 4). During the first 4 days following the pulse, community composition may have affected plot-level GEP. Native grasses composed *ca*. 25% of the low-cover plot canopy cover (Table I) and these had slower photosynthetic development compared to the dominant invasive lovegrass (Figure 3). Early in the monsoon season, native grass A_{net} development generally tracks leaf area growth, whereas the exotic lovegrass maintains green leaves that rapidly uncurl and green up following the first rainfall (Huxman *et al*., 2004; Ignace *et al*., 2007; Hamerlynck *et al*., 2010). Thus, from +1 to +4 days, even though low-cover lovegrass showed more rapid photosynthetic development than in high-cover plots (Figure 3), slower A_{net} development in native grasses may have limited plot-level GEP so that low-cover plot GEP was lower than in high-cover plots on +4 days, and the convergence in GEP on day +7 (Figure 4) may have resulted from similar A_{net} in native grasses and lovegrass at this date (Figure 3). In addition, self-shading, a limitation to productivity and whole-plant carbon gain in other grassland systems (Knapp and Seastedt, 1986; Ryel *et al*., 1993), may have been more common in high-cover gas-exchange plots, resulting in similar GEP between low- and high-cover plots for the 15 days following the rain pulse, when GEP was similar between plots (Figure 4).

Increasing GEP later in the study was not due to changes in leaf-level photosynthesis, as A_{net} was at similar levels across this period and canopy-level photosynthesis (GEP_{lai}) was identical between high- and low-cover plots (Figure 3). Thus, the increases in high-cover GEP (Figure 4) likely reflect increasing proportions of photosynthetically active tissue, even when total canopy LAI (as quantified by the LAI-2000) in the plots did not change substantially across this period (data not shown). This would explain why GEP_{lai} did not differ between plots, and in fact we may have gotten distinctly different GEP_{lai} results if we had been able to scale GEP to green, not total, canopy leaf area (Suyker and Verma, 2001; Hamerlynck *et al*., 2010).

The immediate rise in R_{eco} following rainfall (Figure 4) is likely from soil microbial activity, as roots respond more slowly to rewetting following prolonged dry periods (Jarvis *et al*., 2007). Differences in the magnitude and timing of peak R_{eco} in low- and high-cover plots (Figure 4) may reflect differences in total soluble substrate availability (Davidson *et al*., 2006), or microbial community structure, which may be shaped by past wetting/drying cycles (Fierer *et al*., 2003), and affect R_{eco} flux (Schimel *et al*., 2007; Sponseller, 2007). Such dynamics could influence the controls to Arrhenius-kinematic dynamics that may underlie aridland ecosystem-level pulse responses proposed by Jenerette *et al*. (2008). They suggested energy of activation is lower in high-cover plots, possibly due to more substrate availability or a greater number of viable active sites (Jenerette *et al*., 2008), both of which could be supported by more extensive grass growth. Following this post-rainfall transient, grassland R_{eco} is determined more by root and aboveground plant respiration (Knapp

et al., 1998; Flanagan *et al*., 2002; Flanagan and Johnson, 2005). Thus, the development of higher R_{eco} in high-cover gas-exchange plots is probably due to more extensive root and aboveground growth. Higher R_{eco} in these plots was matched by increasing GEP (Figure 4), whereas in low-cover plots, R_{eco} levelled off as GEP continued to climb (Figure 4). As a result, GEP per unit R_{eco} in low-cover plots was unexpectedly high (Figure 5). It may be that the higher R_{eco} in high-cover plots reflects greater aboveground respiration (Suyker and Verma, 2001; Flanagan and Johnson, 2005), whereas lower R_{eco} in low-cover plots stems from greater contributions from bare soil and reduced aboveground contributions due to less canopy development. It may also be that GEP/R_{eco} follows variation in plant allocation patterns. Controlled glasshouse studies show that desert grassland species alter aboveground/belowground allocation to optimize whole-plant carbon gain with varying moisture (Fernandez and Reynolds, 2000). It may be that previous conditions in low-cover plots resulted in greater allocation to aboveground biomass, resulting in higher GEP/R_{eco} (Figure 5). However, additional aboveground/belowground biomass data are needed to ascertain this.

Even though mid-morning spot NEE measures such as those made here are well correlated with NEE integrated over longer time scales (Hamerlynck *et al*., 2010), extrapolating our results should be made with caution, as differences in short-term measures may not reflect processes expressed over seasonal and inter-annual time spans in pulsed systems such as ours (Reynolds *et al*., 2004). Still, it seems likely that the similar NEE between high- and low-cover conditions (Figure 4) may be a feature in higher net annual productivity seen following experimental rainfall manipulations simulating larger, infrequent events in other semiarid grassland systems (Fay *et al*., 2008; Heisler-White *et al*., 2008, 2009). Such large, saturating rainfall may proportionally increase productivity more in low-cover grassland areas, primarily due to greater internal restraints to R_{eco} (Figure 4), likely stemming from lower total plant biomass. If larger, infrequent storms become more common across western North America (Easterling *et al*., 2000a,b; Seager *et al*., 2007), such constraints may result in more even patterns of productivity across these hydrologically diverse ecological landscapes (Peters *et al*., 2006).

REFERENCES

Christensen JH, Hewitson B. 2007. Regional climate projections. In: *Climate Change 2007: The Physical Science Basis. Contribution of Working Group I to the Fourth Assessment Report of the Intergovernmental Panel on Climate Change*, Solomon S, Qin D, Manning M, Marquis M, Averyt K, Tignor MMB, Miller HL, Chen Z (eds). Cambridge University Press: Cambridge, New York; 487–940.

Comrie AC, Broyles B. 2002. Variability and spatial modeling of fine-scale precipitation data for the Sonoran Desert of southwest Arizona. *Journal of Arid Environments* **50**: 573–592, DOI: 10.1006/jare.2001.0866.

Davidson EA, Janssens IA, Luo Y. 2006. On the variability of respiration in terrestrial ecosystems: moving beyond Q_{10}. *Global Change Biology* **12**: 154–164.

Domingo F, Sanchez G, Moro MJ, Brenner AJ, Puigdefabregas J. 1998. Measurement and modelling of rainfall interception by three semi-arid canopies. *Agricultural and Forest Meteorology* **91**: 275–292.

Easterling DR, Evans JL, Groisman PY, Karl TR, Kunkel KE, Ambenje P. 2000a. Observed variability and trends in extreme climate events: a brief review. *Bulletin of the American Meteorological Society* **81**: 417–425.

Easterling DR, Meehl GA, Parmesan C, Changnon SA, Karl TR, Mearns LO. 2000b. Climate extremes: observations, modeling, and impacts. *Science* **289**: 2068–2074.

Emmerich WE, Verdugo CL. 2008. Precipitation thresholds for CO_2 uptake in grass and shrub communities on Walnut Gulch Experimental Watershed. *Water Resources Research* **44**: W05S16. DOI: 10.1029/2006WR005690.

English NB, Weltzin JF, Fravolini A, Thomas L, Williams DG. 2005. The influence of soil texture and vegetation on soil moisture under rainout shelters in a semi-desert grassland. *Journal of Arid Environments* **63**: 324–343. DOI: 10.1016/j.aridenv.2005.03.013.

Fay PA, Carlisle JD, Knapp AK, Blair JM, Collins SL. 2003. Productivity responses to altered rainfall patterns in a C_4-dominated grassland. *Oecologia* **137**: 245–251. DOI: 10.1007/s00442-003-1331-3.

Fay PA, Kaufman DM, Nippert JB, Carlisle JD, Harper CW. 2008. Changes in grassland ecosystem function due to extreme rainfall events: implications for responses to climate change. *Global Change Biology* **14**: 1600–1608. DOI: 10.1111/j.1365–2486.2008.01605.x.

Fernandez RJ, Reynolds JF. 2000. Potential growth and drought tolerance of eight desert grasses: lack of a trade-off? *Oecologia* **123**: 90–98.

Fierer N, Schimel JP, Holden PA. 2003. Influence of drying-rewetting frequency on soil bacterial community structure. *Microbial Ecology* **45**: 63–71.

Flanagan LB, Johnson BG. 2005. Interacting effects of temperature, soil moisture and plant biomass production on ecosystem respiration in a northern temperate grassland. *Agricultural and Forest Meteorology* **130**: 237–253. DOI: 10.1016/j.agformet.2005.04.002.

Flanagan LB, Wever LA, Carlson PJ. 2002. Seasonal and interannual variation in carbon dioxide exchange and carbon balance in a northern temperate grassland. *Global Change Biology* **8**: 599–615.

Gerten D, Luo Y, LeMarie G, Parton WJ, Keough C, Weng E, Beier C, Ciais P, Cramer W, Dukes JS, Hanson PJ, Knapp AK, Linder S, Nepstad D, Rustad L, Sowerby A. 2008. Modelled effects of precipitation on ecosystem carbon and water dynamics in different climatic zones. *Global Change Biology* **14**: 2365–2379. DOI: 10.1111/j.1365–2486.2008.01651.x.

Gibbens RP, Lenz JM. 2001. Root systems of some Chihuahuan desert plants. *Journal of Arid Environments* **49**: 221–263.

Gómez-Plaza A, Martínez-Mena M, Albaladejo J, Castillo VM. 2001. Factors regulating spatial distribution of soil water content in small semiarid catchments. *Journal of Hydrology* **253**: 211–226.

Goodrich DC, Unkrich CL, Keefer TO, Nichols MH, Stone JJ, Levick LR, Scott RL. 2008. Event to multidecadal persistence in rainfall and runoff in southeastern Arizona. *Water Resources Research* **44**: W05S14. DOI: 10.1029/2007WR006222.

Hamerlynck EP, Scott RL, Moran MS, Keefer TO, Huxman TE. 2010. Growing season ecosystem- and leaf-level gas exchange of an exotic and native semiarid bunchgrass. *Oecologia* **163**: 561–570. DOI: 10.1007/s00442-009-1560-1.

Heisler-White JL, Blair JM, Kelly EF, Harmoney K, Knapp AK. 2009. Contingent productivity responses to more extreme rainfall regimes across a grassland biome. *Global Change Biology* **15**: 2894–2904. DOI: 10.1111/j.1365–2486.2009.01961.x.

Heisler-White JL, Knapp AK, Kelly EF. 2008. Increasing precipitation event size increases aboveground net primary productivity in a semi-arid grassland. *Oecologia* **158**: 129–140. DOI: 10.1007/s00442-008-1116-9.

Hogarth WL, Hopmans J, Parlange JY, Haverkamp R. 1989. Application of a simple soil-water hysteresis model. *Journal of Hydrology* **98**: 21–29.

Huxman TE, Cable JM, Ignace DD, Eilts JA, English NB, Weltzin J, Williams DG. 2004. Response of net ecosystem gas exchange to a simulated precipitation pulse in a semi-arid grassland: the role of native versus non-native grasses and soil texture. *Oecologia* **141**: 295–305. DOI: 10.1007/s0442-003-1389-y.

Ignace DD, Huxman TE, Weltzin JF, Williams DG. 2007. Leaf gas exchange and water status responses of a native and non-native grass to precipitation across contrasting soil surfaces in the Sonoran Desert. *Oecologia* **152**: 401–413. DOI: 10.1007/s.00442-007-0670-x.

Jarvis P, Rey A, Petsikos C, Wingate L, Rayment M, Pereira J, Banza J, David J, Miglietta F, Borghetti M, Manca G, Valentini R. 2007.

Drying and wetting of Mediterranean soils stimulates decomposition and carbon dioxide emission: the "Birch effect". *Tree Physiology* **27**: 929–940.

Jenerette GD, Scott RL, Huxman TE. 2008. Whole ecosystem metabolic pulses following precipitation events. *Functional Ecology* **22**: 924–930. DOI: 10.1111/j.1365–2435.2008.01450.x.

Knapp AK, Beier C, Briske DD, Classen AT, Luo Y, Reichstein M, Smith MD, Smith SD, Bell JE, Fay PA, Heisler JL, Leavitt SW, Sherry R, Smith B, Weng E. 2008. Consequences of more extreme precipitation regimes for terrestrial ecosystems. *Bioscience* **58**: 1–11.

Knapp AK, Conard JL, Blair JM. 1998. Determinants of soil CO_2 flux from a sub-humid grassland: effect of fire and fire history. *Ecological Applications* **8**: 760–770.

Knapp AK, Fahnestock JT, Hamburg SP, Statland LB, Seastedt TR, Schimel DS. 1993. Landscape patterns in soil-plant water relations and primary production in tallgrass prairie. *Ecology* **74**: 549–560.

Knapp AK, Seastedt TR. 1986. Detritus accumulation limits productivity of tallgrass prairie. *Bioscience* **36**: 662–668.

Ludwig JA, Wilcox BP, Breshears DD, Tongway DJ, Imeson AC. 2005. Vegetation patches and runoff-erosion as interacting ecohydrological processes in semiarid landscapes. *Ecology* **86**: 288–297.

Moran MS, Scott RL, Hamerlynck EP, Green KN, Emmerich WE, Holifield-Collins CD. 2009. Evaporative response to Lehmann lovegrass (*Eragrostis lehmanniana*) invasion in a semiarid watershed. *Agricultural and Forest Meteorology* **149**: 2133–2142. DOI: 10.1016/j.agrformet.2009.03.018.

Nearing MA, Kimoto A, Nichols MH. 2005. Spatial patterns of soil erosion and deposition in two small, semiarid watersheds. *Journal of Geophysical Research* **110**: F04020. DOI: 10.1029/2005JF000290.

Nimmo JR, Perkins KS, Schmidt KM, Miller DM, Stock JD, Singha K. 2009. Hydrologic characterization of desert soils with varying degree of pedogenesis: 1. Field experiments evaluating plant-relevant soil water behavior. *Vadose Zone Journal* **8**: 480–495. DOI: 10.2136/vzj2008.0052.

Noy-Meir I. 1973. Desert ecosystems: environment and producers. *Annual Review of Ecology and Systematics* **4**: 25–51.

Ogle K, Reynolds JF. 2004. Plant responses to precipitation in desert ecosystems: integrating functional types, pulses, thresholds, and delays. *Oecologia* **141**: 282–294. DOI: 10.1007/s00442-004-1507-5.

Paige GB, Stone JJ, Smith J, Kennedy JR. 2003. The Walnut Gulch rainfall simulator: a computer-controlled variable intensity rainfall simulator. *Applied Engineering in Agriculture* **20**: 25–31.

Patrick L, Cable J, Potts D, Ignace D, Barron-Gafford G, Griffith A, Alpert H, Van Gestel N, Robertson T, Huxman TE, Zak J, Loik ME, Tissue D. 2007. Effects of an increase in summer precipitation on leaf, soil, and ecosystem fluxes of CO_2 and H_2O in a sotol grassland in Big Bend National Park, Texas. *Oecologia* **151**: 704–718. DOI: 10.1007/s00442-006-0621-y.

Peters DPC, Bestelmeyer BT, Herrick JE, Fredrickson EDL, Monger HC, Havstad KM. 2006. Disentangling complex landscapes: new insights into arid and semiarid system dynamics. *Bioscience* **56**: 491–501.

Potts DL, Huxman TE, Cable JM, English NB, Ignace DD, Eilts JA, Mason MJ, Weltzin JF, Williams DG. 2006. Antecedent moisture and seasonal precipitation influence the response of canopy-scale carbon and water exchange to rainfall pulses in a semi-arid grassland. *New Phytologist* **170**: 849–860. DOI: 10.1111/j.1469–8137.2006.01732.x.

Puigdefabregas J. 2005. The role of vegetation patterns in structuring runoff and sediment fluxes in drylands. *Earth Surface Processes and Landforms* **30**: 133–147.

Reynolds JF, Kemp PR, Ogle K, Fernandez RJ. 2004. Modifying the "pulse-reserve" paradigm for deserts of North America: precipitation pulses, soil water, and plant responses. *Oecologia* **141**: 194–210.

Rhoton FE, Emmerich WE, Goodrich EC, Miller SN, McChesney DS. 2007. An aggregation/erodibility index for soils in a semiarid watershed, Southeastern Arizona. *Soil Science Society of America Journal* **71**: 987–982.

Robertson TR, Zak JC, Tissue DT. 2010. Precipitation magnitude and timing differentially affect species richness and plant density in the sotol grassland of the Chihuahuan Desert. *Oecologia* **162**: 185–197. DOI: 10.1007/s00442-009-1449-z.

Rodriguez-Iturbe I, Porporato A, Ridolfi L, Isham V, Cox DR. 1999. Probabilistic modelling of water balance at a point: the role of climate, soil and vegetation. *Proceedings of the Royal Society of London Series A-Mathematical Physical and Engineering Sciences* **455**: 3789–3805.

Ryel RJ, Beyschlag W, Caldwell MM. 1993. Foliage orientation and carbon gain in two tussock grasses as assessed with a new whole-plant gas-exchange model. *Functional Ecology* **7**: 115–124.

Sanchez G, Puigdefabregas J. 1994. Interactions of plant growth and sediment movement on slopes in a semi-arid environment. *Geomorphology* **9**: 243–260.

Scanlon BR, Levitt DG, Reedy RC, Keese KE, Sully MJ. 2005. Ecological controls on water-cycle response to climate variability in deserts. *Proceedings of the National Academy of Sciences of the United States of America* **102**: 6033–6038. DOI: 10.1073/pnas.0408571102.

Schimel JA, Balser TC, Wallenstein M. 2007. Microbial stress-response physiology and its implications for ecosystem function. *Ecology* **88**: 1386–1394.

Scott RL, Huxman TE, Cable WL, Emmerich WE. 2006. Partitioning of evapotranspiration and its relation to carbon dioxide exchange in a Chihuahuan Desert shrubland. *Hydrological Processes* **20**: 3227–3243. DOI: 10.2002/hyp.6329.

Scott RL, Shuttleworth WJ, Keefer TO, Warrick AW. 2000. Modeling multiyear observations of soil moisture recharge in the semiarid American Southwest. *Water Resources Research* **36**: 2233–2247.

Seager R, Ting M, Held I, Kushnir Y, Lu J, Vecchi G, Huang HP, Harnik N, Leetmaa A, Ngar-Cheung L, Li C, Velez J, Naik N. 2007. Model projections of an imminent transition to a more arid climate in Southwestern North America. *Science* **316**: 1181–1184. DOI: 10.1126/science.1139601.

Seyfried MS, Schwinning S, Wolvoord MA, Pockman WT, Newman BD, Jackson RB, Phillips FM. 2005. Ecohydrological control of deep drainage in arid and semiarid regions. *Ecology* **86**: 277–287.

Sheppard PR, Comrie AC, Packin GD, Angersbach K, Hughes MK. 2002. The climate of the US Southwest. *Climate Research* **21**: 219–238.

Sponseller RA. 2007. Precipitation pulses and soil CO_2 flux in a Sonoran Desert ecosystem. *Global Change Biology* **13**: 426–436. DOI: 10.1111/j.1365–2486.2006.01307.x.

Suyker AE, Verma SB. 2001. Year-round observations of the net ecosystem exchange of carbon dioxide in a native tallgrass prairie. *Global Change Biology* **7**: 279–289.

Wondzell SM, Cunningham GL, Bachelet D. 1996. Relationships between landforms, geomorphic processes, and plant communities on a watershed in the northern Chihuahuan Desert. *Landscape Ecology* **11**: 351–362.